Thermal effects on concrete nanocomposites with central inclined cracks: Influence of crack geometry and nano-SiO₂ content

G. N. Nikolova*

Institute of Mechanics, Bulgarian Academy of Sciences, Sofia, Bulgaria

Received: May 03 2025; Revised: July 11, 2025

This study presents a parametric analysis of the energy release rate (ERR) in concrete nanocomposites containing nano-SiO₂ (1.0%, 1.5%, and 2.0%), with a centrally located crack of varying length and orientation angle (0°, 30°, 45°), under thermal loading. A mathematical model based on linear elastic fracture mechanics (LEFM) was developed, and numerical simulations were performed using Wolfram Mathematica. Thermal stresses were estimated under the assumption of fully constrained thermal expansion, where the temperature rise ΔT is considered as a local uniform increase with respect to a reference state. Only the magnitude of the thermal stress is used in ERR calculations. The study focuses on how ERR values respond to variations in crack geometry, temperature increase, and nanoparticle content. Results indicate that ERR increases with crack length and thermal load but decreases with crack inclination angle. The composite with 1.0% nano-SiO₂ generally exhibits the lowest ERR values in the tested configurations. Although fracture toughness is not experimentally determined in this work, the findings provide a preliminary basis for evaluating the influence of crack geometry and thermal stress on ERR, and for guiding the optimization of thermally resistant concrete nanocomposites.

Keywords: Concrete nanocomposite, 1%, 1.5% and 2% nano-SiO₂, Central crack, LEFM, Numerical results, SIF and ERR

INTRODUCTION

Concrete nanocomposites with added nano-SiO₂ are advanced construction materials that exhibit enhanced mechanical, thermal, and long-term performance compared to ordinary concrete. They are particularly relevant for sustainable and energy-efficient infrastructure, contributing to reduced resource consumption and extended service life [1]. In recent years, numerous studies have focused on the influence of nanoparticles on the mechanical and microstructural properties of concrete [2–8].

The addition of nano-SiO₂ to concrete mixtures leads to an increase in the elastic modulus and a decrease in the coefficient of thermal expansion, which improves the microstructure, enhances density, and reduces porosity, thereby increasing mechanical strength and resistance to cracking.

Thermal loading plays a significant role in crack formation and propagation in concrete structures. While many studies have explored the evaluation of SIF and ERR for various materials, there is still insufficient data on the thermal fracture behavior of nano-SiO₂-modified concrete under idealized thermal conditions, particularly in relation to crack geometry and particle concentration [6, 7, 9, 10].

In this study, thermal stresses are not derived from a real heat conduction problem but are estimated using an idealized approach assuming a uniform temperature increase ΔT throughout the volume, corresponding to a fully constrained expansion scenario. The value of ΔT is interpreted as a local temperature rise with respect to a reference state (e.g., room temperature), not as a vertical temperature gradient. This approximation allows for simplified evaluation of the magnitude of thermal stress and its effect on fracture parameters without resolving the detailed thermal field.

It is important to note that only the absolute value of thermal stress is used in the ERR and SIF calculations, and the influence of restraint conditions is represented in a conservative manner.

Crack geometry, including length and inclination angle, significantly affects stress distribution and crack growth tendencies in nanocomposites.

Analytical and numerical methods for determining stresses, strains, SIF, and ERR are essential for predicting crack initiation and growth, and for evaluating the thermal and mechanical reliability of concrete and other nanostructured materials [11–20].

Reference [11] is a foundational work introducing the concept of SIF and its application to cracks of various geometries. Reference [12] provides key principles of fracture mechanics, including stress concentration analysis and crack propagation. The book [13] discusses fracture mechanics under combined mechanical and thermal

^{*} To whom all correspondence should be sent: E-mail: gery@imbm.bas.bg

stresses, presenting key formulations. Publications [14] and [15] further develop analytical modelling in this field. The handbook [16] offers detailed formulas and examples for SIF calculation, including the effects of temperature-induced stresses. Reference [17] discusses different approaches to modelling thermal—mechanical interactions in cracked materials and computing corresponding SIF values.

Temperature gradients across concrete structures can generate internal thermal stresses that drive crack initiation and growth. Understanding how temperature influences SIF and ERR in nanomodified concrete is essential for assessing its structural reliability and long-term performance.

The formulation used in this study should be viewed as a simplified analytical model aimed at exploring parametric trends under thermal loading, rather than a full representation of thermomechanical coupling in real structures.

The aim of this study is to perform a parametric analysis of the influence of temperature, crack length, and orientation angle, along with different nano-SiO₂ contents, on thermal stress and energy release rate (ERR) in a concrete nanocomposite containing a centrally located inclined crack.

PROBLEM FORMULATION

The geometric model of a concrete nanocomposite with a central inclined crack under monotonic thermal loading ΔT is presented in Figure 1.

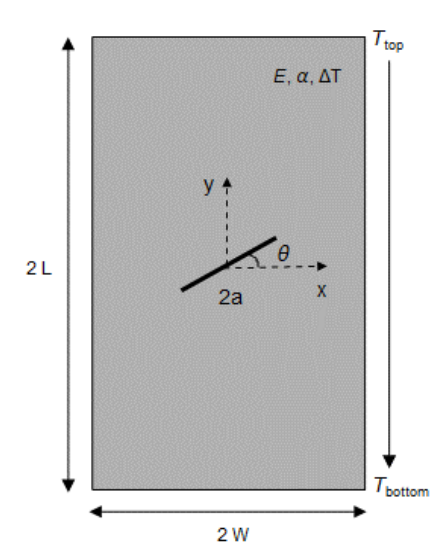


Figure 1. Geometric model of a concrete nanocomposite with a centrally located inclined crack under monotonic thermal loading ΔT .

The nanocomposite is modelled as a rectangular plate with width 2W, length 2L and a central crack with length 2a, oriented at an angle θ relative to the

horizontal x-axis. The x and y axes of the Oxy coordinate system used in the model are represented by dashed lines, with the origin positioned at the midpoint of the crack. The x-axis spans the width $(x \in [-W, W])$, and the y-axis spans the height of the plate $(y \in [-L, L])$, with the positive y-direction pointing upwards.

The thermal loading ΔT is defined as a temperature difference between the top surface (T_{top}) and the bottom surface (T_{bottom}) , i.e., $\Delta T = T_{top} - T_{bottom}$.

In the numerical model, this is treated as a vertical thermal gradient, which induces internal thermal stresses due to constrained thermal expansion of the material.

In contrast, the analytical model interprets ΔT as a local, uniform temperature rise at the crack location, relative to a reference state (e.g., ambient temperature). Under the assumption of fully restrained thermal expansion, this approximation allows for simplified estimation of the thermal stress magnitude and its effect on fracture parameters. This modelling approach is conservative and commonly used for preliminary parametric analysis. The direction of the temperature gradient is indicated in Figure 1.

The coordinate system is centered at the midpoint of the crack. In the case of a horizontal crack ($\theta = 0^{\circ}$), the geometry is symmetric with respect to both axes. For inclined cracks ($\theta > 0^{\circ}$), symmetry with respect to the x-axis is preserved, but the overall geometry becomes asymmetric, particularly in terms of heat transfer, which is considered in the numerical analysis.

The orientation angle θ is defined as the angle between the crack line and the horizontal axis (x-axis), measured in a counterclockwise direction. In this configuration, $\theta = 0^{\circ}$ corresponds to a horizontal crack perpendicular to the vertical thermal gradient. In the present analysis, three angles are considered: $\theta = 0^{\circ}$, 30° , and 45° , representing increasing crack inclination relative to the temperature gradient direction. These configurations are illustrated schematically in Figure 1.

BASIC EQUATIONS

Thermal stress

The thermal stress induced by the load is determined by Hooke's law using the following expression:

$$\sigma_T = E. \alpha . \Delta T$$
 (1)

where σ_T denotes the thermal stress, E is the modulus of elasticity of the concrete nanocomposite,

 α - the coefficient of linear thermal expansion, and ΔT is the difference in temperatures of the top and bottom surfaces of the concrete nanocomposite.

Equation (1) provides an approximate estimation of the thermal stress magnitude under the assumption that the entire body is fully constrained and cannot expand. In such a case, the total strain ε_{total} equals zero, and thermal stress develops internally due to restrained expansion. The full expression from elasticity theory, $\sigma = E(\varepsilon_{total} -$ $\alpha . \Delta T$), simplifies to equation (1) when $\varepsilon_{total} = 0$. In this study, only the magnitude of the thermal stress is used in the calculations of the stress intensity factor and energy release rate, the sign is not considered. This assumption corresponds to an idealized boundary condition commonly adopted in fracture mechanics analyses of massive concrete or ceramic structures under thermal loading. Although such full restraint may not occur in real engineering conditions, it provides a conservative estimate of internal stress and is widely used for parametric evaluation in early-stage modelling [13-16].

Stress intensity factor and energy release rate

• SIF calculation. The mathematical model for calculating the stress near the crack tip (SIF) as a function of the orientation angle of the central crack θ can be described using equations from LEFM, [11-15].

For a rectangular plate with finite dimensions (length 2L and width 2W), containing a central crack of length 2a and orientation angle θ relative to the load, the stress intensity factor K_I is determined by:

$$K_I = \sigma_T \cdot \sqrt{\pi a} \cdot Y(a, \theta) \tag{2}$$

where a is half the length of the crack, and $Y(a, \theta)$ is a geometric correction function that accounts for both the relative crack size and its inclination. While this formulation is traditionally derived for mechanical tensile loading, it is applied here by substituting the magnitude of the thermally induced stress σ_T , to allow for parametric comparison of thermal fracture behaviour. The correction function is expressed as:

$$Y(a,\theta) = \frac{1}{\sqrt{\cos(\frac{\pi a}{2W})}} \cdot F(\theta)$$
 (3)

This form is constructed by analogy with classical Mode I SIF formulations for finite-width plates under mechanical loading. The term $\frac{1}{\sqrt{cos(\frac{\pi a}{2W})}}$

is used to approximate the effect of finite plate geometry, while the angular factor $cos^2\theta$ represents the reduction in the Mode I opening component as

the crack becomes more inclined. Although these terms are not derived from thermal fracture theory, they enable a simplified parametric evaluation of the trends in thermal fracture behavior under varying geometries. This heuristic approach offers practical insight, but it should not be interpreted as a rigorous solution based on thermomechanical coupling. The angular correction factor $F(\theta)$ is given by:

$$F(\theta) = \cos^2 \theta \tag{4}$$

This expression is based on the projection of normal stress components acting perpendicular to the crack plane, and it is consistent with tensor transformation results for inclined cracks.

This angular correction factor is introduced heuristically in the present study and appears here for the first time in this specific thermal fracture context.

Equations (3) and (4) are valid only within certain geometric limits: for small crack lengths relative to the plate width $a \ll W$, and moderate inclination angles $\theta < 75^{\circ}$. For $a \to W$ or $\theta \to 90^{\circ}$, the correction function becomes singular or unphysical. These cases are therefore excluded from the present analysis.

By combining equations (1), (3), and (4), the final expression for the stress intensity factor becomes:

$$K_I = \sigma_T . \sqrt{\pi a} . \frac{1}{\sqrt{\cos(\frac{\pi a}{2W})}} . \cos^2 \theta \tag{5}$$

This allows evaluation of how crack length, orientation, and thermal loading affect the intensity of the local stress field near the crack tip.

Although the expression originates from tensile loading conditions, its use here with thermal stress serves as an approximation to analyze relative trends in fracture behavior under idealized thermal conditions.

It should be noted that the expression in eq. (5) is not a direct result from classical thermal fracture theory. Rather, it is constructed by analogy with mechanical LEFM models, using heuristic correction factors to account for finite geometry and crack inclination. This formulation represents the author's contribution for enabling a simplified parametric analysis under thermal loading conditions.

As the crack length increases, the SIF K_I grows approximately with a, modulated by the geometric correction factor. Similarly, the crack orientation reduces the effective stress component through the $\cos^2\theta$ term.

The addition of nano-SiO₂ modifies both the elastic modulus E and the thermal expansion coefficient α , which directly affects the value of σ_T ,

and thus influences both the SIF K_I and the energy release rate G.

Although inclined cracks generally experience mixed-mode loading (Modes I and II), in this study only the Mode I SIF is considered for simplicity, based on the assumption that the dominant contribution to crack propagation arises from opening mode stresses due to constrained thermal expansion.

• *ERR calculation*. The energy release rate (ERR) is a key parameter in fracture mechanics, reflecting the energy available for crack propagation. It represents the rate at which elastic strain energy is released per unit crack extension and is particularly relevant for assessing the potential for thermally induced fracture in brittle materials such as concrete nanocomposites.

Once the stress intensity factor K_I has been calculated, ERR can be determined using:

$$G = \frac{K_L^2}{E} \tag{6}$$

This relation is derived under the assumption of Mode I crack propagation and plane stress conditions, which are appropriate for thin plates or surface cracks. It provides a scalar measure of the energy concentration at the crack tip.

In this study, the ERR is not interpreted as an absolute criterion for crack growth, but rather as a comparative parameter to evaluate the influence of different input variables (crack length, orientation, thermal load, and nano-SiO₂ content).

It should be noted that fracture toughness - i.e., the critical value of *G* required for crack propagation - is not experimentally measured here. Therefore, the ERR values are not used to directly predict failure, but to identify parametric trends and material configurations that reduce the energy available for crack advancement.

This approach aligns with the theoretical objective of the work and supports the preliminary assessment of thermally resistant nanocomposite design.

ANALYTICAL AND NUMERICAL SOLUTIONS

A hybrid analytical - numerical methodology was used to calculate the thermal stress, the stress intensity factor K_I , and the energy release rate G in a concrete nanocomposite with a centrally located inclined crack under thermal loading.

In this context, 'hybrid' refers to the combination of analytical fracture mechanics expressions with numerically computed temperature fields. The analytical expressions are used to calculate fracture parameters (thermal stress, K_I , and G), while the

numerical model is employed solely to evaluate the temperature distribution and validate the assumptions about local thermal loading.

Analytical expressions based on linear elastic fracture mechanics (LEFM) were implemented in Wolfram Mathematica using custom-developed macros. These allow for systematic and automated evaluation of fracture-related parameters across a wide range of input variables, including crack length α , orientation angles θ , thermal gradients ΔT , and material parameters E and α , corresponding to 1.0%, 1.5%, and 2.0% nano-SiO₂ content.

Thermal stress was calculated under the idealized assumption of fully restrained thermal expansion, leading to conservative estimates of internal stresses. This approximation allows for simplified trend analysis without solving a full thermal—mechanical coupling problem.

The resulting values of K_I and G were determined using the corrected geometric functions and were interpreted for comparative purposes.

In parallel, numerical simulations were carried out to visualize the applied temperature field and to examine the effects of crack geometry and thermal loading on the fracture parameters.

The results were presented using 2D and 3D parametric plots, which illustrate how ERR depends on crack geometry, temperature variation, and material stiffness. This method provides an efficient and accessible tool for preliminary thermal fracture assessment in nanocomposite materials, avoiding the complexity of full-scale finite element modelling.

Mechanical and thermal properties of the concrete composite

The mechanical and thermal properties of the concrete nanocomposites with different nano-SiO₂ contents used in the calculations and simulations, are summarized in Table 1. These values are based on experimentally validated literature data and are assumed constant throughout the simulations [1-6].

Table 1. Mechanical and thermal properties of the concrete nanocomposite

Type of concrete nanocomposite	Elastic modulus, E [GPa]	Coefficient of thermal expansion, $\alpha [1/K]$
with 1% nano-SiO ₂	40	9.5×10^{-6}
with 1.5% nano-SiO ₂	42	9.3×10^{-6}
with 2% nano-SiO ₂	43	9.2×10^{-6}

These input parameters directly affect the computed thermal stress and thus influence the stress intensity factor and energy release rate.

Assumed values for the temperature ΔT and geometry

The geometric configuration and thermal loading parameters used in the simulations are summarized in Table 2. The rectangular concrete nanocomposite plate is assumed to have a centrally located inclined crack, with variations in both crack geometry and thermal input. These parameters are applied consistently in the analytical model (for calculating thermal stress, K_I and G) and in the numerical simulations (for evaluating the thermal field and geometric effects).

Table 2. Geometric and thermal parameters used in the simulations

Thermal load, $\Delta T [K]$	20 ÷ 100
Plate length, 2L [m]	1
Plate width, 2W [m]	0.5
Initial crack length, $2a [m]$	$0.01 \div 0.1$
Orientation angle, θ [°]	0 ÷ 45

The thermal loading ΔT is interpreted in two distinct but consistent ways: In the analytical approach, ΔT is considered a local uniform temperature rise relative to a reference state (e.g., ambient temperature), corresponding to a fully constrained thermal expansion scenario. In the numerical model, it is treated as a vertical temperature gradient applied from the top to the bottom of the plate, representing practical thermal loading conditions in structural elements.

These ranges ensure that the analytical formulas remain within valid geometric bounds, avoiding singularities in the correction functions for large $\frac{a}{W}$ or extreme values of θ . The selected parameter space enables the observation of key trends in energy release rate and fracture sensitivity under varying thermal and geometric configurations.

The range of ΔT is selected to encompass typical and elevated service conditions for concrete structures, ensuring that the model captures conservative thermal stress effects.

Temperature distribution at different orientation angles. Calculation of thermal stress

Numerical macros were developed in Wolfram Mathematica to simulate the temperature distribution in a cracked concrete nanocomposite with different crack orientation angles θ . In parallel, analytical calculations of the thermal stress were carried out using equation (1) under the assumption of fully constrained thermal expansion.

In the numerical model, the geometry of the rectangular plate (length 2L and width 2W) and the central crack (length 2a and orientation angle θ) are first defined. Material properties for the different nanocomposites, including Young's modulus and thermal expansion coefficient, are taken from Table 1. The applied thermal load corresponds to a temperature difference $\Delta T = 100 K$, as specified in Table 2.

The boundary conditions for the thermal model are defined as follows: fixed temperatures are applied to the top and bottom surfaces using Dirichlet conditions: $T[x, -L] = T_{bottom} = 400 \text{ K}$ and $T[x, L] = T_{top} = 300 \text{ K}$. This imposes a vertical temperature gradient along the y-axis. The lateral boundaries $x = \pm W$ are thermally insulated, represented by natural Neumann conditions (zero heat flux): $\frac{\partial T(x,y)}{\partial y} = 0$, at $x = \pm W$. At the crack surfaces $(x = \pm a)$, an adiabatic condition is assumed, meaning that the heat flux across the crack faces is zero: $\frac{\partial T(x,y)}{\partial y} = 0$ at $x = \pm a$. The steadystate temperature field is obtained by solving the Laplace equation using the finite element method $\frac{\hat{\partial}^2 T(x,y)}{\partial x^2} + \frac{\partial^2 T(x,y)}{\partial y^2} = 0.$ The numerical (FEM): solution of the Laplace equation was performed in Wolfram Mathematica using its built-in finite element method (FEM) framework. The domain was discretized using an adaptive unstructured mesh of second-order triangular elements (ElementOrder → 2), which provide higher accuracy for smooth solutions such as temperature fields. The mesh was refined near the crack zone to better capture local temperature gradients. Dirichlet and Neumann boundary conditions were directly imposed using the DirichletCondition and NeumannValue functions. The software's built-in NDSolveValue was used to solve the steady-state heat conduction problem.

The simulations are performed for a fixed crack length of $2a = 0.1 \, m$ and $\Delta T = 100 \, K$, while the crack orientation angle is varied ($\theta = 0^{\circ}, 30^{\circ}, 45^{\circ}$). In contrast, the analytical thermal stress is computed from the simplified expression $\sigma_T = E.\alpha.\Delta T$, assuming uniform temperature rise at the crack location with respect to a reference temperature. This approach provides an upper-bound estimate of internal stress under fully restrained expansion.

As shown in Figure 2, when the crack orientation is horizontal ($\theta = 0^{\circ}$), the temperature distribution in the nanocomposite remains relatively uniform, indicating a more balanced heat transfer and a lower concentration of thermal stresses near the crack.

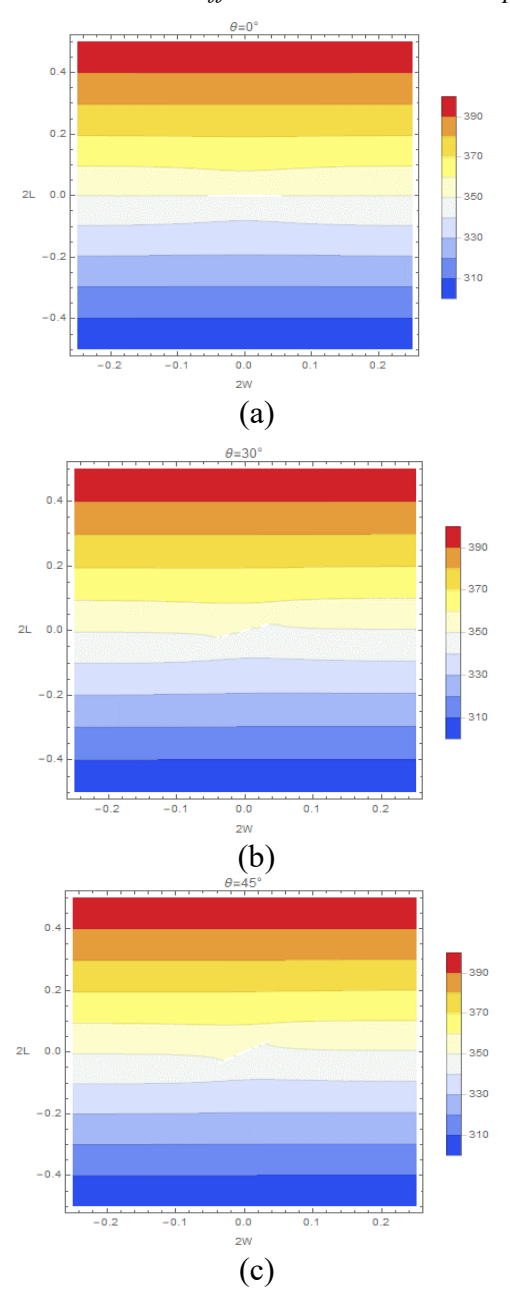


Figure 2. Temperature distribution in a concrete nanocomposite at different crack orientation angles: (a) $\theta = 0^{\circ}$; (b) $\theta = 30^{\circ}$; (c) $\theta = 45^{\circ}$

In contrast, for inclined cracks ($\theta > 30^{\circ}$), the temperature field becomes increasingly distorted in the vicinity of the crack. The inclination leads to asymmetric heat flow, which creates steeper local temperature gradients near the crack tips. These gradients are associated with higher thermal stresses due to restricted expansion in those regions. The numerical model presented here is used solely to compute the temperature field and to examine how crack orientation affects the local thermal distribution. It is not used to compute thermal stresses or fracture parameters. Instead, it serves as a visual justification for the use of a local ΔT assumption in the analytical solution near the crack

zone. It should be noted that the temperature value at the crack location (e.g., $\approx 350 \, K$ in Figure 2) reflects the mid-point of the linear temperature gradient between the top $(400 \, K)$ and bottom $(300 \, K)$ boundaries. This value is consistent with the global temperature difference $\Delta T = 100 \, K$ used in both the numerical and analytical models. In the analytical approach, ΔT is interpreted as a local uniform increase relative to a reference temperature, enabling estimation of thermal stress through equation (1).

The thermal stress σ_T increases linearly with temperature difference ΔT , according to eq. (1), and is used as input for subsequent SIF and ERR calculations. Adding a higher percentage of nano-SiO₂ to the concrete composite enhances its mechanical and thermal properties, including increased stiffness (elastic modulus) and improved thermal conductivity. However, this modification also intensifies the development of thermal stresses within the material. At elevated temperatures, the enhanced thermal conductivity leads to faster heat transfer, which steepens the internal temperature gradient. Under constrained conditions, this steeper gradient results in greater thermally induced stresses, especially near stress concentrators such as cracks.

Analytical and numerical solution for ERR

After obtaining the analytical solutions for the thermal stresses, macros were generated in the Wolfram Mathematica software to calculate both K_I and G for various crack configurations- specifically, different crack lengths a and orientation angles θ in a concrete nanocomposite with different percentages of nano-SiO₂.

Using the basic analytical equations, the fracture parameters were computed for each case. Additionally, 3D parametric plots were generated based on the analytical formula to study the dependence of ERR on crack length, orientation angle, K_I , elastic modulus E, and the thermal load ΔT . These simulations allowed for the systematic assessment of how changes in temperature gradient and material stiffness affect the energy release rate.

The results provide insight into the parametric influence of nano-SiO₂ content and thermal loading on thermal fracture behavior. Higher values of ΔT and crack inclination generally resulted in increased ERR, indicating greater risk of crack propagation under thermal stress.

• Analytical solution for ERR. Figure 3 illustrates the dependence of the energy release rate G on the stress intensity factor K_I for a concrete nanocomposite containing 1.0% nano-SiO₂. The values of K_I and G are calculated for a fixed

temperature difference $\Delta T = 50 \, K$, for various crack lengths $a = 0.005 \div 0.050 \, m$ and crack orientation angles $\theta = 0^{\circ}, 30^{\circ}, 45^{\circ}$.

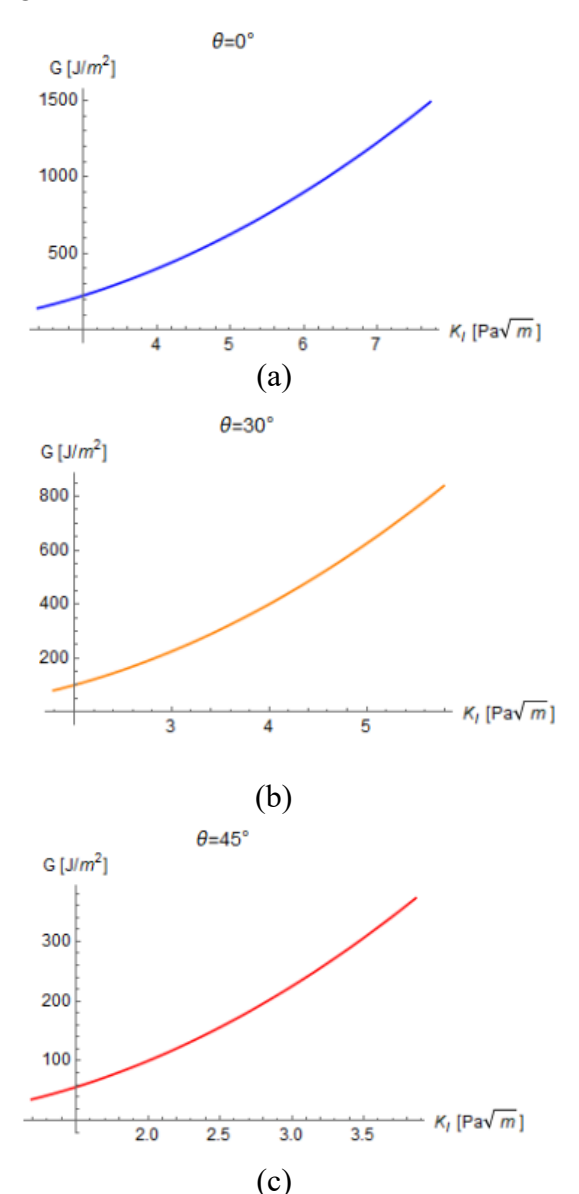


Figure 3. Dependence of the energy release rate G on the stress intensity factor K_I at different crack orientation angles: (a) $\theta = 0^{\circ}$; (b) $\theta = 30^{\circ}$; (c) $\theta = 45^{\circ}$

For a fixed crack orientation angle, both K_I and G increase with increasing crack length, following the square-root dependence on a and the geometric correction factors. Longer cracks concentrate higher thermal stresses at the crack tip, making them more susceptible to propagation under thermal loading. Conversely, for a fixed crack length, increasing the inclination angle θ leads to a noticeable decrease in both K_I and G. The lowest values are observed at $\theta = 45^{\circ}$, due to the reduced effective stress component acting normal to the crack plane. This behavior is consistent with fracture mechanics theory, where inclined cracks experience a reduced

driving force for Mode I opening under vertically directed thermal stress. This inverse relationship between crack angle and ERR highlights the importance of crack orientation in the design of thermally resistant nanocomposite structures.

• Numerical modelling of energy release rate at different crack angles and lengths. Figure 4 illustrates the variation of the energy release rate G for different crack orientation angles $\theta = (0^{\circ} \div 45^{\circ})$ and crack lengths $a = 0.005 \div 0.05m$, at a fixed temperature difference $\Delta T = 50 \ K$.

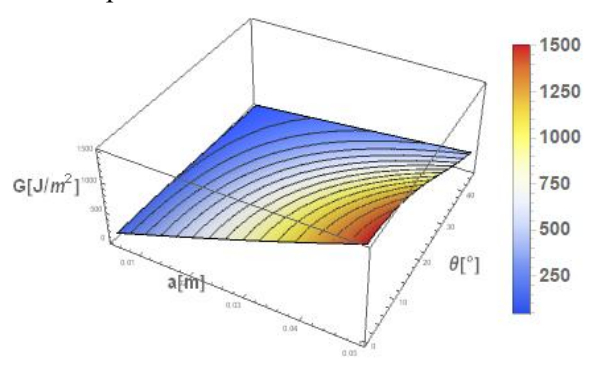


Figure 4. Dependence of *G* on crack orientation angle θ and crack length α at $\Delta T = 50$ K.

The results demonstrate that at a fixed crack angle θ , increasing the crack length a leads to a significant rise in G. Conversely, for a fixed crack length, increasing θ reduces the value of G, with minimum ERR observed at $\theta = 45^{\circ}$. This trend is consistent with the analytical form of the angular correction factor $F(\theta) = cos^2\theta$ which decreases with higher inclination angles, reducing the component of thermal stress acting normal to the crack.

These findings confirm that crack geometry - especially length and inclination - has a stronger effect on ERR than nano-SiO₂ content. Nevertheless, for composites with higher stiffness (e.g., 2.0% nano-SiO₂), ERR values remain higher due to increased thermal stress magnitudes under the same ΔT .

• 3D simulation of the dependence of ERR on SIF and the elastic modulus. With increasing nano-SiO₂ content (1.5% and 2%), the elastic modulus E of the concrete nanocomposite increases, resulting in higher thermal stresses under the same temperature gradient. Consequently, the stress intensity factor K_I and the energy release rate G also increase, as illustrated in Figure 5. However, the influence of crack orientation shows the opposite trend: for fixed crack length, increasing the inclination angle θ leads to a decrease in both K_I and G. This is due to the reduction in the normal component of thermal stress acting on the crack plane.

G. Nikolova: Thermal effects on concrete nanocomposites with central inclined cracks: Influence of crack geometry ...

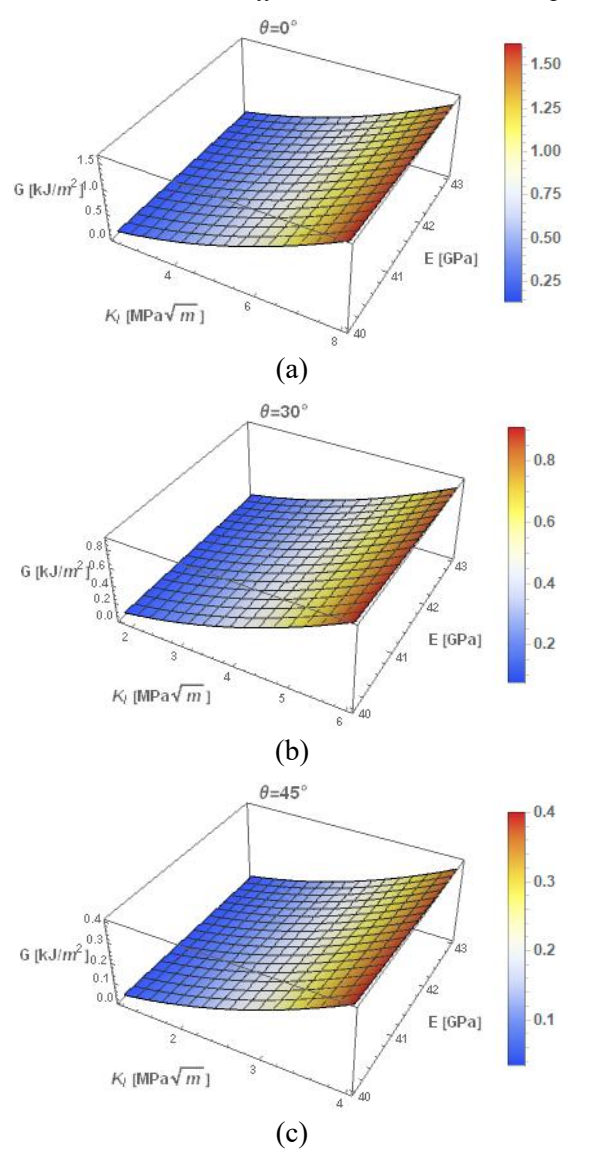


Figure 5. Dependence of *G* on K_I and *E* for $\Delta T = 50 K$.

Overall, higher nanoparticle content increases the material's stiffness and thermal stress, promoting crack propagation, while greater crack inclination angles tend to stabilize the crack by lowering the energy available for its growth.

• Numerical modelling of ERR at different ΔT . At temperature differences $\Delta T > 80 \, K$, the concrete nanocomposite with 2% nano-SiO₂ exhibits a pronounced increase in the energy release rate G, indicating a higher susceptibility to thermally induced crack propagation, Figure 6. This behavior reflects the increased stiffness of the material, which leads to higher thermal stresses under constrained conditions. In contrast, the composite with 1% nano-SiO₂ maintains the lowest values of G across the considered range of ΔT , suggesting improved resistance to thermal cracking.

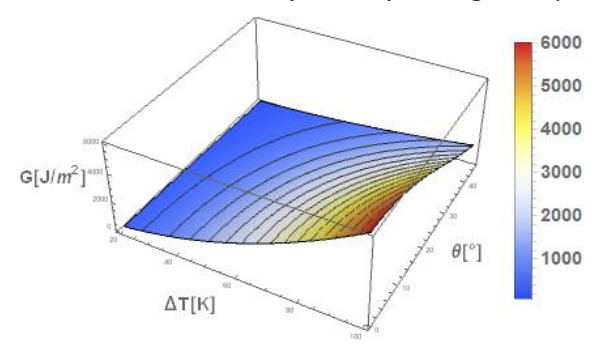


Figure 6. Dependence of G on ΔT and θ for a = 0.05 m

The influence of the crack inclination angle θ is also significant: for a fixed crack length, ERR values decrease with increasing angle, confirming the stabilizing effect of inclined cracks under thermal loading. The numerical results are in good agreement with the analytical model and support the conclusion that both thermal load intensity and crack geometry critically affect fracture behavior in nanomodified concrete.

INFERENCES FROM THE OBTAINED ANALYTICAL AND NUMERICAL RESULTS

Based on the conducted analytical and numerical study, the following conclusions can be drawn:

- The addition of nano-SiO₂ affects both the mechanical and thermal fracture behavior of concrete nanocomposites. At 1.0% content, the material demonstrates the lowest energy release rate values across a wide range of crack lengths and orientation angles, indicating improved thermal crack resistance.
- For fixed crack orientation angles, both the stress intensity factor K_I and the energy release rate G increase with crack length, and this growth is more pronounced at higher elastic moduli (i.e., higher nano-SiO₂ content). However, for fixed crack lengths, increasing the crack inclination angle leads to a significant reduction in both K_I and G, with the lowest values observed at $\theta = 45^{\circ}$, confirming the stabilizing effect of inclined cracks under thermal loading.
- Numerical simulations confirm the analytical predictions and provide detailed 2D and 3D visualizations of how ERR varies with crack length, angle, elastic modulus, and thermal load. The results highlight that crack geometry has a stronger influence on ERR than nanoparticle content under moderate thermal gradients.
- At elevated thermal loads ($\Delta T > 80 K$), concrete with 2.0% nano-SiO₂ shows a sharp rise in ERR, indicating increased brittleness and risk of thermal crack propagation despite its higher stiffness. This suggests a trade-off between stiffness

enhancement and fracture resistance at higher nanoparticle concentrations.

• For thermally and mechanically reliable design, it is crucial to optimize the nano-SiO₂ content. A 1.0% addition appears to provide a favorable compromise, especially for structures exposed to moderate thermal gradients and at risk of fracture initiation due to thermal loading.

It is important to note that the study is based on a simplified analytical model assuming fully constrained thermal expansion and using only the magnitude (not the sign) of thermal stress. No experimental fracture toughness measurements were conducted. The conclusions are therefore applicable to preliminary design and parametric assessment purposes and should be validated with further experimental data.

CONCLUSION

In this study, a mathematical model based on elastic fracture mechanics (LEFM) was developed to determine the energy release rate (ERR) in a concrete nanocomposite containing different percentages of nano-SiO₂ (1%, 1.5%, and 2%) under monotonic thermal loading. The analysis focused on evaluating the influence of crack length and orientation angle on thermally induced damage processes in concrete.

Thermal stress was estimated using a simplified analytical expression, assuming fully restrained thermal expansion and considering only the magnitude of the stress, without accounting for its sign. While this approach does not yield exact stress distributions, it provides a practical approximation suitable for comparative parametric analysis of ERR and SIF values.

Numerical simulations carried out in Wolfram Mathematica enabled the evaluation of ERR across a wide range of temperature differences and crack configurations. The results demonstrate that ERR increases with thermal load and crack length, but decreases with increasing crack inclination angle, especially beyond 30°. Among the studied compositions, concrete with 1.0% nano-SiO₂ exhibited the most favorable behavior, with the lowest ERR across most conditions. In contrast, higher nanoparticle contents (1.5% and 2%) were associated with higher ERR at large crack lengths, particularly under high temperature gradients, due to the increased elastic modulus and resulting thermal stresses.

The developed model provides a useful framework for the preliminary evaluation and design of thermally resistant concrete nanocomposites. However, it should be noted that the analysis does

not include experimental determination of fracture toughness, and the results are valid within the limitations of the adopted assumptions. Future work will focus on validating the proposed analytical model through comparison with experimental data and high-fidelity numerical simulations using commercial FEM software, to further assess the model's predictive capability.

REFERENCES

- M. Alvansazyazdi, F. Alvarez-Rea, J. Pinto-Montoya, M. Khorami, P. Bonilla-Valladares, A. Debut, M. Feizbahr, Sustainability, 15(21), 1 (2023).
- 2. M. Lezgy-Nazargah, S. Emamian, E. Aghasizadeh et al., *Sādhanā*, **43**, 196 (2018).
- 3. H. Hamadi, R. Atea, S. Badr, *International Journal of Applied Sciences and Technology*, **4(3)**, 234 (2022).
- 4. S. Aleem, M. Heikal, W. Morsi, *Construction and Building Materials*, **59**, 151 (2014).
- 5. G. Vasanth, K. Ramadevi, *International Journal of Advanced Research in Science, Communication and Technology*, 50 (2022).
- D. Syamsunur, L. Wei, Z. Memon, S. Surol, N. Yusoff, *Materials*, 15(20), 7073 (2022).
- 7. P. Brzozowski, J. Strzałkowski, P. Rychtowski, R. Wróbel, B. Tryba, E. Horszczaruk, *Materials*, **15(1)**, 166 (2022).
- 8. F. Sanchez, K. Sobolev, *Construction and Building Materials*, **24** (11), 2060 (2010).
- 9. A. Kizilkanat, N. Yüzer, N. Kabay, *Construction and Building Materials*, **45**, 157 (2013).
- 10. Q. Ma, R. Guo, Z. Zhao, Z. Lin, K. He, *Construction and Building Materials*, **93**, 371 (2015).
- 11. G. Irwin, *Journal of Applied Mechanics*, **24(3)**, 361 (1957).
- 12. T. Anderson, Fracture Mechanics: Fundamentals and Applications, 4th edn., CRC Press, 2017.
- 13. Z. Bazant, J. Planas, Fracture and Size Effect in Concrete and Other Quasibrittle Materials, 1st edn., Routledge, (1998).
- 14. P. Paris, F. Erdogan, *Journal of Basic Engineering*, **85(4)**, 528 (1963).
- 15. M. Williams, Journal of Applied Mechanics, **24(1)**, 10 (1957).
- H. Tada, P. Paris, G. Irwin, The Stress Analysis of Cracks Handbook, 3rd edn., ASME Press, 2000, p. 698.
- 17. G. Sih, Mechanics of Fracture, 1. Noordhoff International Publisher, Leyden, (1973).
- 18. A. Yanakieva, G. Nikolova, *Journal of Theoretical and Applied Mechanics*, **50**, 389 (2020).
- 19. A. Yanakieva, *International Journal of Mechanical and Production Engineering (IJMPE)*, **3(11)**, 47 (2015).
- 20. T. Petrova, *Bulgarian Chemical Communications*, **55(3)**, 349 (2023).